

Iterative Learning Impedance Control Based on Physical Recovery Condition Elevation

He Jinbao^{*1,2}, Zhuge Xia¹, Luo Zaifei¹, Li Guojun¹, Zhang Yinchun²

¹School of Electronic and Information Engineering, Ningbo University of Technology, No.89 Cuibai Road, Haishu District, Ningbo, Zhejiang, China, Ph.: 0086-0574-87081231

²Department of Biomedical Engineering, University of Houston, 3605 Cullen Blvd, Houston, TX 77204

*Corresponding author, e-mail:perfecthjb@126.com

Abstract

Rehabilitation robots have been designed to improve ability of patients with impaired limbs to perform activities of daily life. A new iterative learning impedance control (ITLC) algorithm was developed in the present study based on the physical recovery condition of impaired limbs to improve the performance of rehabilitation robots. The physical recovery condition elevation of impaired limbs was first evaluated in terms of periodic force and trajectory tracking ratio (TTR) parameters, and the desired impedance was then modified on line using the fuzzy method according to the change of physical recovery condition. Secondly, an adaptive impedance controller was designed and modified using the iterative learning method. The convergence was analyzed based upon the Lyapunov-like positive definite sequence, which was monotonically decreasing under the proposed control schemes. Finally, the simulation experiments were conducted to compare the proposed ITLC approach the traditional impedance control. Results demonstrate the effectiveness of our learning impedance controller in rehabilitative training.

Keywords: rehabilitation robot, physical recovery, condition elevation, impedance control, iterative learning

Copyright © 2014 Institute of Advanced Engineering and Science. All rights reserved.

1. Introduction

As the population of many countries around the world is aging, people suffered stroke get more and more, especially those who are in their old age. The patients with stroke may occur neurological defects, and the limb movement handicap is the most common type, which is one of the real problems. In the past few years, the rehabilitation of limb movement has received much attention [1, 2]. Repetitive movements can improve muscular strength of patients with impairments due to neurological or orthopedic problems. It's an urgent problem that how to improve the daily life activity of patients with central nervous system injury caused by cerebrovascular diseases. The development of rehabilitation exoskeletons can solve it. The impaired limb cannot supply enough strength to complete repetitive movements, and exoskeleton rehabilitation robot has been designed to assist the impaired limb. Increasing evidence suggests that rehabilitation robot with the motor control can simplify position and force control tasks. The designs of robot controller have been studied by many researchers [3, 4], which can be used for reference.

To design rehabilitation robot controller is one of the most important tasks and major difficulties. In recent years, a lot of researches have been focused on control system design of rehabilitation training robot, which mainly includes force control methods, that concerns the impedance property between robot and impaired limb. Impedance control is one of the main robot force control methods. F. Caccavale et al [5] described the definition of the elastic contribution in the impedance equation according to the task requirements, and used an energy based argument to derive the dynamic equation of a mechanical impedance characterized by a translational part and a rotational part. Seul Jung et.al [6] proposed a new simple and stable force tracking impedance control scheme that has the capability to track a specified desired force and to compensate for uncertainties of environment location and stiffness. E. Akdogan et al. [7] designed a device for rehabilitation of lower extremities and implemented impedance force control between robot and knee arthrosis. S. H. Kang et al [8] developed an accurate and

robust impedance control technique based on internal model control structure and time-delay estimation to solve the trade-off problem between impedance accuracy and robustness against modeling error. Patel R.V., et al [9] designed an outer-inner loop controller, that is, the augmented hybrid impedance control scheme, which concerns robust position and contact force control for robot arms. However, most impedance controllers are implemented with constant desired parameters. When the environment condition changed, the impedance controller with fixed impedance parameters is not effective [10].

The classical linear controllers are not easy to satisfy the requirements of practical use because the practical situations generally depend on impaired limb's physical recovery. We should adjust the controllers during rehabilitation training process. Since repetitive tasks are generally used in rehabilitation training robots, we should take advantage of the fact that the reference trajectory is repeated over a given operation time. The iterative learning control (ILC) techniques can be applied in order to enhance the tracking performance. Kaneko K. et al. [11] described repetitive motion control schemes for rigid-link robot manipulators. The control objective was to track a prescribed desired trajectory which was periodic and required repeated learning trials. Bukkems B. et al. [12] proposed a combination method of ILC and model-based control to achieve high-quality motion control of direct-drive robots in repetitive motion tasks. On one hand, model-based and learning components compensate much of the nonlinear and coupled robot dynamics. On the other hand, the ILC algorithm using Lyapunov and Lyapunov-like methods has been developed. In the papers of Xu and Tan [13], and Xu [14], the ILC algorithms have been proposed based upon the use of a positive definite Lyapunov-like sequence. In contrast to the standard adaptive control, this technique is shown to be able to handle systems with time-varying parameters. Based on this approach, Abdelhamid Tayebi [15] proposed adaptive ILC schemes for trajectory tracking of rigid robot manipulators, by performing repetitive tasks. The base of ILC is the use of a proportional-derivative feedback structure. Visoli A. et al [16] proposed a new method based on an ILC algorithm for industrial robot manipulator, which considered hybrid force/velocity control (both implicit and explicit) and was improved by repeating the task. However, for rehabilitation robot, the physical recovery condition of impaired limb is hard to get.

There have been some researches on combination the impedance control and iterative learning theory. Pham Thuc Anh Nguyen et al. [17] proposed an iterative learning control scheme for impedance control of robotic tasks when the characteristics of reproducing force of the deformable material was nonlinear in its displacement. Tsuji T et al. [18] developed a new method to regulate the impedance parameter of the end-effector through learning of neural networks. Chien-Chern Cheah [19] put forward a method for analyzing the convergence of the learning impedance system. Byungchan Kim [20] proposed a learning strategy of motor skill for robotic contact tasks based on a human motor control theory and machine learning schemes. However, it is difficult to provide a theoretical framework for rehabilitation robot system, and to guarantee the convergence and guide the applications of such formulations.

The purpose of this paper is to present a novel adaptive impedance controller for rehabilitation robot which is modulated by iterative learning algorithm with the progress of the therapy. We also describe a fuzzy method that modulates the impedance error of track and force between the limbs and robot. Finally, it is verified that the impedance error converges to zero.

This paper is organized as follows. Section 2 describes the methods for evaluating impaired limb's physical recovery condition, and introduces the fuzzy method for modulating the impedance error according to impaired limb's physical recovery condition. In section 3, we design the iterative learning impedance controller for rehabilitation robot. Moreover, the convergence of the closed loop system is proven using the Lyapunov function to guarantee the global convergence of tracking error. In section 4, simulation results of traditional impedance control and ILIC are presented and discussed, which shows our designed controller provides good dynamic control performance in terms of the change of the impaired limb's physical condition.

2. Research Method

2.1. Physical Recovery Condition Elevation of Impaired Limb

In the present study, so-called robot-aided training strategies are used in the rehabilitation of patients that involve recognizing the patient's movement intention in terms of muscular efforts, feedbacking the information to the patient and adapting the robotic assistance to the patient's contribution. The best control strategy should be implemented to assist patients with their movements only as much as necessary. So, at first, we should get the patient's movement intention, then the rehabilitation robot controller is designed to avoid limb being hurt again.

However, there are two situations that we don't want to meet. One is that the patient's intention is to move while the impaired limb can't move in term of its physical recovery condition; The other is that the patient wants to stop while the impaired limb is able to move. Then the training intensity of impaired limb is not enough. In view of this, the impaired limb physical recovery condition can not be negligible, that is, we should consider both patient's intention and impaired limb's physical recovery condition. By now, a few of researchers have focused on this problem.

Some mechanical parameters of the impaired limb have been used to evaluate its physical recovery condition [21, 22], but the mechanical parameters, such as damp, stiffness, may introduce false estimation when muscle spasm occurs. D.J. Bennett has proved through experiments that the arm mechanical properties were time-varying during ongoing arm movement [23].

In this paper, we present $\bar{\omega}_{ke}$ (the periodic force error between robot and impaired limb) and TTR (trajectory tracking ratio) to estimate the impaired limb's physical recovery condition. Since these coefficients are obtained in one movement period, it may avoid unusual situations affecting the final judgment, such as muscle spasm and stiff. Figure 1 gives the block diagram of proposed ILIC system which is mainly composed of estimation of impaired limb and iterative learning. In order to improve the effectiveness of recovery training, we modify the reference force on line according to the estimation of impaired limb, and design impedance controller with iterative learning method.

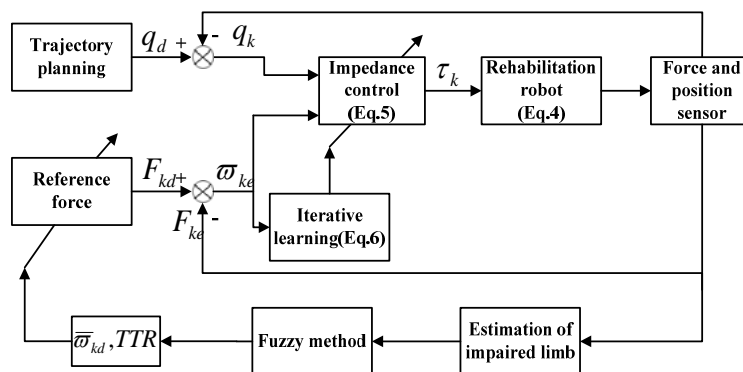


Figure 1. Block Diagram of ILIC System

The target impedance between robot and impaired limb is expressed [21] by:

$$M_d \ddot{X}_{ke}(t) + C_d \dot{X}_{ke}(t) + K_d \ddot{X}_{ke}(t) = F_{kd} - F_k = F_{ke}(t) \quad (1)$$

Where $X_{ke} = q_d(t) - q_k(t)$, M_d , C_d and $K_d \in R^n$ are positive definite matrices which specify the desired dynamic relationship between the reference position error and the interaction force, and $q_d, q_k \in R^n$ are the reference position and real position, respectively. F_{kd} and F_k are the desired force and real force, respectively.

To obtain the reasonable impedance, the target impedance should be modulated according to the impaired limb. The target impedance can be described as:

$$F_{kd} = (1 + \varepsilon) F_{(k-1)d} \quad (2)$$

Where F_{kd} , $F_{(k-1)d}$ are the k -th and $(k-1)$ -th target impedance, and $\varepsilon \in [-0.5, 0.5]$ is the adjustment factor on impaired limb condition. $F_{ke} = F_{kd} - F_k$, F_k is the actual force.

The impedance error is defined as:

$$\varpi_{ke} = M_d X_{ke}(t) + C_d \dot{X}_{ke}(t) + K_d \ddot{X}_{ke}(t) - F_{ke}(t) \quad (3)$$

In order to improve the robustness and practicability of the algorithm, we use parameters of TTR and \bar{F}_k to estimate the impaired limb's physical recovery condition. The TTR can be obtained by actual trajectory length divided by total trajectory length in one periodic movement. The \bar{F}_k can be given by:

$$\bar{F}_k = \frac{1}{T} \sum_{k=1}^N \bar{F}_k$$

Where T is the time of one periodic movement, and \bar{F}_k is the real force of robot's end-effector obtained from the force sensor. The changes of \bar{F}_k ($\Delta\bar{F}_k$) and TTR (ΔTTR) are used as inputs of fuzzy controller, and the desired impedance is used as the output, namely, $\Delta\varepsilon$. All these inputs and output variables are scaled and mapped to five Gaussian membership functions, namely, negative big (NB), negative small (NS), zero (ZE), positive small (PS) and positive big (PB), respectively. Membership function of every variables is defined as Gauss function. Table 1 is the fuzzy rules between inputs ($\Delta\bar{F}_k$ and ΔTTR) and output.

Table 1. Fuzzy Rules

$\Delta\varepsilon$		ΔTTR				
		NB	NS	ZR	PS	PB
$\Delta\bar{F}_k$	NB	PB	PB	PB	PS	ZR
	NS	PB	PB	PS	ZR	NS
	ZR	PB	PS	ZR	NS	NB
	PS	PS	ZR	NS	NB	NB
	PB	ZR	NS	NB	NB	NB

In general, the patient's movement intention can improve the movement ability of the impaired limb, which shows in the changes of \bar{F}_k ($\Delta\bar{F}_k$) and TTR (ΔTTR). Therefore, the desired impedance can be turned according to the impaired limb physical recovery condition regardless of patient's intention.

2.2. Iterative Learning Impedance Control

In this section, we present the iterative learning impedance control (ILIC) algorithm for rehabilitation robot. Impedance controllers are well designed in the field of interaction of robotics and human-system and applied in robot-aided upper extremity therapy of stroke patients [24]. The basic idea of the ILIC strategy applied to robot-aided training is to allow a variable deviation from a predefined limb trajectory rather than impose a rigid pattern. This amount of deviation depends on the patient's effort and behavior. An adjustable time is applied at each joint in order to keep the limb within a defined range centered on the predefined trajectory.

2.2.1. System Model

Using the Lagrangian formulation and considering the contact force and the constraints, the motion of the constrained rehabilitation robot is expressed by the following equation with degrees of freedom.

$$M(q_k)\ddot{q}_k(t) + C(q_k, \dot{q}_k)\dot{q}_k(t) + G(q_k) = \tau_k + \tau_d \quad (4)$$

Where $q_k, \dot{q}_k, \ddot{q}_k \in R^n$ are the robot joint position, joint velocity and robot joint acceleration vectors, respectively. $M(q_k) \in R^{n \times n}$ is the inertia matrix. $C(q_k, \dot{q}_k)\dot{q}_k \in R^n$ contains the centrifugal Coriolis and centrifugal forces. $G(q_k) \in R^n$ is the vector resulting from the gravitational forces. $\tau_k \in R^n$ is the control input vector containing the torques to be applied at each joint. $\tau_d \in R^n$ denotes the vector containing the external torque and un-modeled disturbances.

Assuming that joint positions and joint velocities are available for the feedbacks from sensors, our objective is to design a control law τ_k to guarantee the boundedness of $q_k(t)$ and $\varpi_{ke}(t), t \in [0, T]$. $\varpi_{ke}(t)$ converges to zero and $q_k(t)$ converges to the desired reference trajectory $q_d(t)$ for $\forall t \in [0, T]$ when k tends to infinity.

We assume that the rehabilitation robot has the following properties which are common to robot manipulators.

(A1) $M(q_k) \in R^{n \times n}$ is symmetric, bounded, and positive definite.

(A2) The matrix $\dot{M}(q_k) - 2C(q_k, \dot{q}_k)$ is skew symmetric, and $\dot{M}(q_k) = 2C(q_k, \dot{q}_k)$.

(A3) $G(q_k) + C(q_k, \dot{q}_k)\dot{q}_d(t) = \eta(q_k, \dot{q}_k)\zeta^T(t)$, where $\eta(q_k, \dot{q}_k) \in R^{n \times (m-1)}$ is a known matrix and $\zeta(t) \in R^{m-1}$ is an unknown continuous vector over $[0, T]$.

(A4) $\|C(q_k, \dot{q}_k)\| \leq k_c \|\dot{q}_k\|, \|G(q_k)\| < k_g, \forall t \in [0, T]$ and $\forall k \in \mathbb{N}_+$, where k_c and k_g are unknown positive parameters.

For rehabilitation robot, we make the following reasonable assumptions:

(B1) The reference trajectory and its 1st and 2nd time-derivative, namely q_d, \dot{q}_d and \ddot{q}_d , as well as the τ_d and target impedance F_{kd} , are bounded for $\forall t \in [0, T]$, and $\|M(q_k)\ddot{q}_k - \tau_d\| \leq \alpha, \alpha > 0$.

(B2) The resetting condition is satisfied, that is, $q_d(0) - q_k(0) = \dot{q}_d(0) - \dot{q}_k(0) = 0, \forall k \in \mathbb{N}_+$

(B3) $\|(M \cdot M_d + C \cdot C_d)C\ddot{q}_d - M^{-1}d_k\| \leq \sigma, \sigma > 0$

2.2.2. Iterative Learning Impedance Controller (ILIC)

In this section, we present the iterative learning impedance controller (ILIC) for rehabilitation robot.

Theorem 1: Consider rehabilitation robot system (4) with properties (A1-A4) and assumptions (B1-B3) under the following control law:

$$\tau_k(t) = M[K_p \varpi_{ke}(t) + C\dot{\varpi}_{ke}(t) + \hat{\sigma}_k(t) \text{sgn}(\dot{\varpi}_{ke}(t))] \quad (5)$$

With,

$$\hat{\sigma}_k(t) = \hat{\sigma}_{k-1}(t) + \rho \dot{\varpi}_{ke}^T \text{sgn}(\dot{\varpi}_{ke}(t)) \quad (6)$$

Let $\Gamma \leq \rho^T \text{sgn}(\varpi_{ke}) \text{sgn}(\varpi_{ke})^T$, and $\Gamma = k_c (\|\dot{q}_d\|)_{\max}$ be satisfied, then $\lim_{k \rightarrow \infty} \varpi_{ke} = \lim_{k \rightarrow \infty} \dot{\varpi}_{ke} = 0$, $\lim_{k \rightarrow \infty} \tilde{q}_k = \lim_{k \rightarrow \infty} \dot{\tilde{q}}_k = 0$. In control law (5), (6), $\sigma_k(t) = [\zeta^T(t) \ \sigma]^T$, and $\hat{\sigma}(t)$ is the estimation value of $\theta(t)$ that $\hat{\theta}_{-1}(0) = 0$. The matrix $\phi(\varpi_{ke}, \dot{\varpi}_{ke}) \in R^{n \times n}$ is defined as $\phi(\varpi_{ke}, \dot{\varpi}_{ke}) = [\eta(q_k, \dot{q}_k) \ \text{sgn}(\dot{\tilde{q}}_k)]$, where $\text{sgn}(\cdot)$ is the signum function. The matrix $K_p \in R^{n \times n}$, $\rho \in R^{n \times n}$ are symmetric positive definite.

2.2.3. Proof of This Theorem

The proof of this theorem is in three steps. The first step is to prove that the positive definite Lyapunov-like function is non-increasing and bounded with respect to k . In the second step, we show that the resetting value of Lyapunov-like function is bounded for all $t \in [0, T]$. In the—last step, we get the results, that is, $\lim_{k \rightarrow \infty} \varpi_{ke} = \lim_{k \rightarrow \infty} \dot{\varpi}_{ke} = 0$, $\lim_{k \rightarrow \infty} \tilde{q}_k = \lim_{k \rightarrow \infty} \dot{\tilde{q}}_k = 0$

(1) Step 1: Choose the following Lyapunov-like composite energy function

$$V_k(\varpi_{ke}, \dot{\varpi}_{ke}, \tilde{\sigma}_k) = U_k(\varpi_{ke}, \dot{\varpi}_{ke}) + \frac{1}{2} \int_0^t \tilde{\sigma}_k(\tau) \rho^{-1} \tilde{\sigma}_k(\tau) d\tau \quad (7)$$

Where $\tilde{\sigma}_k(t) = \sigma(t) - \hat{\sigma}_k(t)$

The term $U_k(\varpi_{ke}, \dot{\varpi}_{ke})$ in (7) is written as:

$$U_k(\varpi_{ke}, \dot{\varpi}_{ke}) = \frac{1}{2} \varpi_{ke}^T K_p \varpi_{ke} + \frac{1}{2} \dot{\varpi}_{ke}^T M(q_k) \dot{\varpi}_{ke} \quad (8)$$

The difference of V_k is given by:

$$\Delta V_k = V_k - V_{k-1} = U_k - U_{k-1} + \frac{1}{2} \int_0^t (\tilde{\sigma}_k^T(\tau) \rho^{-1} \tilde{\sigma}_k(\tau) - \tilde{\sigma}_{k-1}^T(\tau) \rho^{-1} \tilde{\sigma}_{k-1}(\tau)) d\tau \quad (9)$$

Define $\hat{\sigma}_k(t) = \tilde{\sigma}_{k-1}(t) - \tilde{\sigma}_k(t)$, then:

$$\tilde{\sigma}_{k-1}(t) = \hat{\sigma}_k(t) + \tilde{\sigma}_k(t) \quad (10)$$

Using (10), we have:

$$\begin{aligned} \int_0^t (\tilde{\sigma}_k^T(\tau) \rho^{-1} \tilde{\sigma}_k(\tau) - \tilde{\sigma}_{k-1}^T(\tau) \rho^{-1} \tilde{\sigma}_{k-1}(\tau)) d\tau &= \int_0^t (\tilde{\sigma}_k^T \rho^{-1} \tilde{\sigma}_k - (\hat{\sigma}_k + \tilde{\sigma}_k)^T \rho^{-1} (\hat{\sigma}_k + \tilde{\sigma}_k)) d\tau \\ &= \int_0^t [-(\hat{\sigma}_k^T \rho^{-1} \hat{\sigma}_k + \hat{\sigma}_k^T \rho^{-1} \tilde{\sigma}_k + \tilde{\sigma}_k^T \rho^{-1} \hat{\sigma}_k)] d\tau = \int_0^t [-(\hat{\sigma}_k^T \rho^{-1} \hat{\sigma}_k + 2\tilde{\sigma}_k^T \rho^{-1} \hat{\sigma}_k)] d\tau \end{aligned}$$

Hence,

$$\Delta V_k = U_k - U_{k-1} - \frac{1}{2} \int_0^t (\hat{\sigma}_k^T \rho^{-1} \hat{\sigma}_k + 2\tilde{\sigma}_k^T \rho^{-1} \hat{\sigma}_k) d\tau \quad (11)$$

For,

$$\int_0^t \dot{U}_k(\tau) d\tau = U_k(t) - U_k(0)$$

Hence,

$$U_k(t) = U_k(0) + \int_0^t \dot{U}_k(\tau) d\tau$$

While,

$$\dot{U}_k(t) = \dot{\omega}_{ke}^T K_P \varpi_{ke} + \dot{\omega}_{ke}^T M(q_k) \ddot{\omega}_{ke} + \frac{1}{2} \dot{\omega}_{ke}^T \dot{M}(q_k) \dot{\omega}_{ke} \quad (12)$$

Therefore,

$$U_k(t) = U_k(0) + \int_0^t (\dot{\omega}_{ke}^T K_P \varpi_{ke} + \dot{\omega}_{ke}^T M(q_k) \ddot{\omega}_{ke} + \frac{1}{2} \dot{\omega}_{ke}^T \dot{M}(q_k) \dot{\omega}_{ke}) d\tau \quad (13)$$

Consider the rehabilitation robot system property that the movement speed is slow, we can obtain:

$$\varpi_{ke} \approx M_d \dot{X}_{ke}(t) + C_d \dot{X}_{ke}(t) - F_{ke}(t) \quad (14)$$

$$\dot{\varpi}_{ke} \approx M_d \ddot{X}_{ke}(t) - \dot{F}_{ke}(t) \quad (15)$$

$$\ddot{\varpi}_{ke} \approx M_d \ddot{\ddot{X}}_{ke}(t) - \ddot{F}_{ke}(t) \quad (16)$$

Using (14), (15), (16) and (4) in (12), in view of (A2), we obtain:

$$\begin{aligned} \dot{U}_k(t) &= \dot{\omega}_{ke}^T K_P \varpi_{ke} + \dot{\omega}_{ke}^T M(q_k) \ddot{\omega}_{ke} + \frac{1}{2} \dot{\omega}_{ke}^T \dot{M}(q_k) \dot{\omega}_{ke} \\ &= \dot{\omega}_{ke}^T (K_P \varpi_{ke} + M(q_k) \ddot{\omega}_{ke} + \frac{1}{2} \dot{M}(q_k) \dot{\omega}_{ke}) \\ &\approx (M_d \dot{X}_{ke} - \dot{F}_{ke})^T (K_P (M_d \dot{X}_{ke} + C_d \dot{X}_{ke} - F_{ke}) + M(q_k) (M_d \ddot{X}_{ke} - \ddot{F}_{ke})) \\ &\quad + \frac{1}{2} \dot{M}(q_k) (M_d \dot{X}_{ke} - \dot{F}_{ke}) - C \dot{F}_{ke} - M \ddot{F}_{ke} \end{aligned} \quad (17)$$

While $X_{ke} = q_d(t) - q_k(t)$, hence:

$$\begin{aligned} \dot{U}_k(t) &\approx \dot{\omega}_{ke}^T [(M \cdot M_d + C \cdot C_d) C \ddot{q}_d + M^{-1} (C \dot{q}_d + G - \tau_k - \tau_d)] \\ &\quad + K_P M_d \dot{X}_{ke} - K_P F_e + (C M_d + K_P C_d) \dot{X}_{ke} - C \dot{F}_{ke} - M \ddot{F}_{ke} \end{aligned} \quad (18)$$

According to assumption B3, we obtain:

$$\dot{\omega}_{ke}^T [(M \cdot M_d + C \cdot C_d) C \ddot{q}_d - M^{-1} d_k] \leq \|\dot{\omega}_{ke}^T\| \alpha = \dot{\omega}_{ke}^T \alpha \operatorname{sgn}(\dot{\omega}_{ke}^T) \quad (19)$$

Using (18), (19) and property (A3), we obtain:

$$\int_0^t \dot{U}_k d\tau \leq \int_0^t \dot{\omega}_{ke}^T [K_P \varpi_{ke} + C \dot{\omega}_{ke} - M^{-1} \tau_k + \alpha \operatorname{sgn}(\dot{X}_{ke}) + M^{-1} \eta^T] d\tau \quad (20)$$

Since,

$$\phi = [\eta(q_k, \dot{q}_k) \quad \operatorname{sgn}(\dot{\omega}_{ke})], \quad \sigma_k(t) = \begin{bmatrix} \zeta^T(t) \\ \sigma \end{bmatrix}$$

We obtain in view of (10):

$$\int_0^t \dot{U}_k(\tau) d\tau \leq \int_0^t \dot{\bar{w}}_{ke}^T [K_P \bar{w}_{ke} + C \dot{\bar{w}}_{ke} - M^{-1} \tau_k + \phi \sigma_k] d\tau \quad (21)$$

Substituting control law (5) into(13), hence:

$$U_k(t) \leq U_k(0) + \int_0^t \dot{\bar{w}}_{ke}^T \cdot (\tilde{\sigma}_k \operatorname{sgn}(\dot{\bar{w}}_{ke}) + \Gamma \dot{\bar{w}}_{ke}) d\tau \quad (22)$$

Substituting control law (22) into(11), we obtain:

$$\begin{aligned} \Delta V_k &= U_k - U_{k-1} - \frac{1}{2} \int_0^t (\tilde{\sigma}_k^T \rho^{-1} \tilde{\sigma}_k + 2\tilde{\sigma}_k^T \rho^{-1} \tilde{\sigma}_k) d\tau \\ &\leq -U_{k-1} + \int_0^t [\dot{\bar{w}}_{ke}^T \cdot (\tilde{\sigma}_k \operatorname{sgn}(\dot{\bar{w}}_{ke}) + \Gamma \dot{\bar{w}}_{ke}) - \frac{1}{2} \tilde{\sigma}_k^T \rho^{-1} \tilde{\sigma}_k - \tilde{\sigma}_k^T \rho^{-1} \tilde{\sigma}_k] d\tau \end{aligned} \quad (23)$$

From (6), we obtain:

$$\tilde{\sigma}_k^T \rho^{-1} \tilde{\sigma}_k = \dot{\bar{w}}_{ke} \rho^T \operatorname{sgn}(\dot{\bar{w}}_{ke}) \operatorname{sgn}(\dot{\bar{w}}_{ke}) \dot{\bar{w}}_{ke}^T \quad (24)$$

$$\tilde{\sigma}_k^T \rho^{-1} \tilde{\sigma}_k = \dot{\bar{w}}_{ke}^T \tilde{\sigma}_k \operatorname{sgn}(\dot{\bar{w}}_{ke}) \quad (25)$$

Substituting (24), (25) into (23), so:

$$\begin{aligned} \Delta V_k &= U_k - U_{k-1} - \frac{1}{2} \int_0^t (\tilde{\sigma}_k^T \rho^{-1} \tilde{\sigma}_k + 2\tilde{\sigma}_k^T \rho^{-1} \tilde{\sigma}_k) d\tau \\ &\leq -U_{k-1} + \int_0^t [\dot{\bar{w}}_{ke}^T \cdot (\tilde{\sigma}_k \operatorname{sgn}(\dot{\bar{w}}_{ke}) + \Gamma \dot{\bar{w}}_{ke}) - \frac{1}{2} \tilde{\sigma}_k^T \rho^{-1} \tilde{\sigma}_k - \tilde{\sigma}_k^T \rho^{-1} \tilde{\sigma}_k] d\tau \\ &\leq -U_{k-1} - \frac{1}{2} \int_0^t \dot{\bar{w}}_{ke}^T \cdot (\rho^T \operatorname{sgn}(\dot{\bar{w}}_{ke}) \operatorname{sgn}(\dot{\bar{w}}_{ke}) - \Gamma) \dot{\bar{w}}_{ke} d\tau \end{aligned} \quad (26)$$

While $\Gamma \leq \rho^T \operatorname{sgn}(\dot{\bar{w}}_{ke}) \operatorname{sgn}(\dot{\bar{w}}_{ke})^T$, one can obtain:

$$\Delta V_k \leq 0$$

Therefore, the Lyapunov function $V_k(\bar{w}_{ke}, \dot{\bar{w}}_{ke}, \tilde{\sigma}_k)$ is non-increasing.

(2) Step 2: This step is to prove that $V_k(\bar{w}_{ke}, \dot{\bar{w}}_{ke}, \tilde{\sigma}_k)$ is continuous and bounded when $k = 0$.

Chose $k = 0$, we obtain:

$$\begin{aligned} \dot{V}_0 &\leq \dot{\bar{w}}_0^T \cdot (\tilde{\sigma}_0 \operatorname{sgn}(\dot{\bar{w}}_0) + \Gamma \dot{\bar{w}}_0) + \frac{1}{2} \tilde{\sigma}_0^T \rho^{-1} \tilde{\sigma}_0 \\ &\leq |\dot{\bar{w}}_0| \tilde{\sigma}_0 + \dot{\bar{w}}_0^T \Gamma \dot{\bar{w}}_0 + \frac{1}{2} \tilde{\sigma}_0^T \rho^{-1} \tilde{\sigma}_0 \end{aligned}$$

For $2ab \leq a^2 + b^2$

Then,

$$|\dot{\bar{w}}_0| \tilde{\sigma}_0 \leq \frac{1}{2} (\dot{\bar{w}}_0^2 + \tilde{\sigma}_0^2)$$

Hence,

$$\begin{aligned} \dot{V}_0 &\leq |\dot{\tilde{w}}_0| \tilde{\sigma}_0 + \dot{\tilde{w}}_0^T \Gamma \dot{\tilde{w}}_0 + \frac{1}{2} \tilde{\sigma}_0^T \rho^{-1} \tilde{\sigma}_0 \\ &\leq \frac{1}{2} (\|\dot{\tilde{w}}_0\|^2 + \|\tilde{\sigma}_0\|^2) + \lambda_{\max}(\Gamma) \|\dot{\tilde{w}}_0\|^2 + \frac{1}{2} \lambda_{\max}(\rho^{-1}) \|\tilde{\sigma}_0\|^2 \\ &\leq \frac{1}{2} (1 + 2\lambda_{\max}(\Gamma)) \|\dot{\tilde{w}}_0\|^2 + \frac{1}{2} (1 + 2\lambda_{\max}(\rho^{-1})) \|\tilde{\sigma}_0\|^2 \end{aligned}$$

$\lambda_{\max}(\bullet)$ is the max eigenvalue of (\bullet) , therefore, $V_0(t)$ is continuous and bounded.

(3) Step 3: To prove the Continuity and boundedness of $V_k(t)$

$V_k(t)$ can be rewritten as:

$$V_k(t) = V_0 + \sum_{j=1}^k \Delta V_j$$

From (26), we can obtain:

$$\sum_{j=1}^k \Delta V_j \leq -\sum_{j=1}^k U_{j-1}$$

And,

$$V_k(t) \leq V_0 - \sum_{j=1}^k U_j \leq V_0 - \frac{1}{2} \sum_{j=1}^k [\dot{\tilde{w}}_{je}^T K_p \tilde{w}_{je} + \dot{\tilde{w}}_{je}^T M \dot{\tilde{w}}_{je}]$$

Therefore:

$$\frac{1}{2} \sum_{j=1}^k [\dot{\tilde{w}}_{je}^T K_p \tilde{w}_{je} + \dot{\tilde{w}}_{je}^T M \dot{\tilde{w}}_{je}] \leq V_0 - V_k \leq V_0$$

That is, $V_k(t)$ is continuous and bounded.

From the Step 1, Step 2 and Step 3, we can obtain that $\lim_{k \rightarrow \infty} \tilde{w}_{ke} = \lim_{k \rightarrow \infty} \dot{\tilde{w}}_{ke} = 0$,

$$\lim_{k \rightarrow \infty} \tilde{q}_k = \lim_{k \rightarrow \infty} \dot{\tilde{q}}_k = 0, \quad \forall t \in [0, T]$$

3. Simulation Results

For two-joint rehabilitation robot, the system model can be written as:

$$M(q_k) \ddot{q}_k(t) + C(q_k, \dot{q}_k) \dot{q}_k(t) + G(q_k) = \tau_k + \tau_d$$

Where,

$$\begin{aligned} M(q_k) &= \begin{bmatrix} m_{11} & m_{12} \\ m_{21} & m_{22} \end{bmatrix}, \quad C(q_k, \dot{q}_k) = \begin{bmatrix} c_{11} & c_{12} \\ c_{21} & c_{22} \end{bmatrix} \\ m_{11} &= m_1 l_{c1}^2 + m_2 (l_1^2 + l_{c2}^2 + 2l_1 l_{c2} \cos q_2) + I_1 + I_2 \\ m_{12} &= m_{21} = m_2 (l_{c2}^2 + l_1 l_{c2} \cos q_2) + I_2 \end{aligned}$$

$$\begin{aligned}
 m_{22} &= m_2 l_{c2}^2 + I_2 \\
 c_{11} &= -m_2 l_1 l_{c2} \sin q_2 \cdot \dot{q}_2 \\
 c_{12} &= -m_2 l_1 l_{c2} \sin q_2 \cdot (\dot{q}_1 + \dot{q}_2) \\
 c_{21} &= m_2 l_1 l_{c2} \sin q_2 \cdot \dot{q}_1 \\
 G(q_k) &= \begin{bmatrix} (m_1 l_{c1} + m_2 l_1) g \cos q_1 + m_2 l_{c2} g \cos(q_1 + q_2) \\ m_2 l_{c2} g \cos(q_1 + q_2) \end{bmatrix}
 \end{aligned}$$

$\tau_d = [d_m \sin t \quad d_m \cos t]^T$, where d_m is random signal with amplitude 1.

The parameters of rehabilitation robot are chosen as $m_1 = m_2 = 1$, $l_1 = l_2 = 0.5$, $l_{c1} = l_{c2} = 0.2$, $I_1 = I_2 = 0.05$.

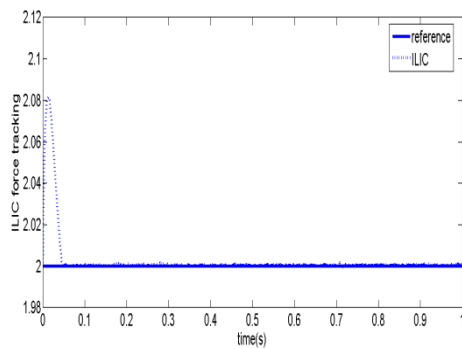


Figure 2. Constant Force Tracking Using ILIC

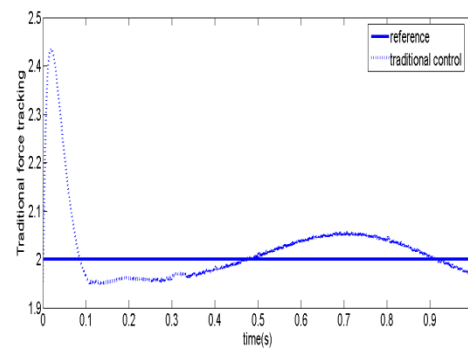


Figure 3. Constant Force Tracking Using Traditional Control

For constant force tracking, the desired positions of two joints are $qd1 = \sin(2\pi t)$, and $qd2 = \cos(2\pi t)$. To guarantee the same between desired positions and real outputs at the beginning, the real output is set to be $S(0) = 2$. With the control law (5), (6), and the resetting condition, and $K_p = 12 \cdot eye(2)$, $\rho = 15$, $M_d = C_d = 1$, $K_d = 0.5$, we get the constant force $F_{kd} = 2$. The starting state of joint1 and joint2 is $S'(0) = [0 \quad 0 \quad 1 \quad 0]^T$, which refers to the position and speed of joint1 and joint2, that is $S'(0) = [position \quad speed \quad position \quad speed]^T$.

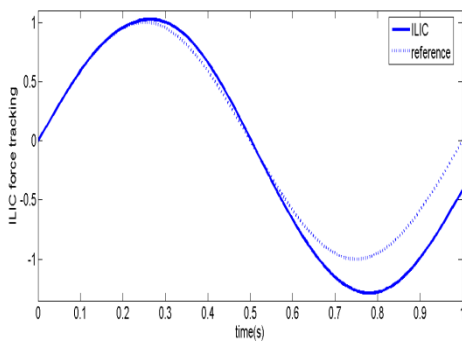


Figure 4. The Variable Force Tracking of the First Iteration

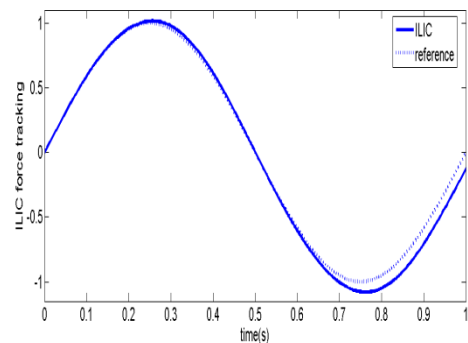


Figure 5. The Variable Force Tracking of the Third Iteration

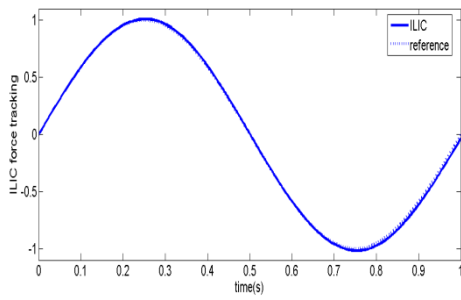


Figure 6. The Variable Force Tracking of the Fifth Iteration

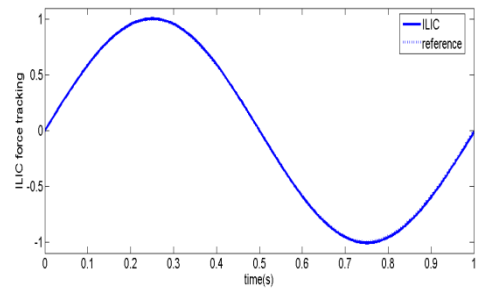


Figure 7. The Variable Force Tracking of the Eighth Iteration

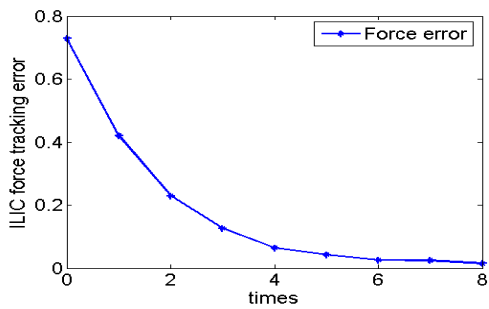


Figure 8. The Variable Force Tracking Error of Iterative Process

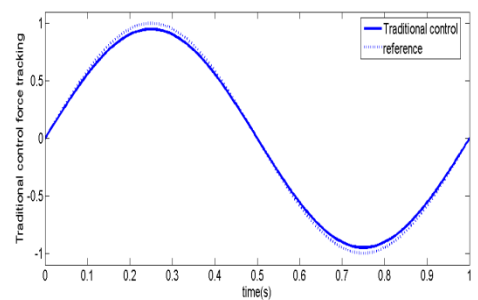


Figure 9. The Variable Force Tracking Using Traditional Impedance Control

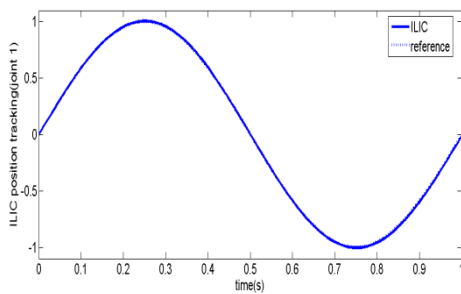


Figure 10. The Position Tracking Using ILIC of Joint1

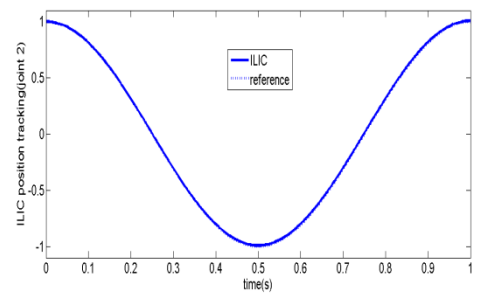


Figure 11. The Position Tracking Using ILIC of Joint2

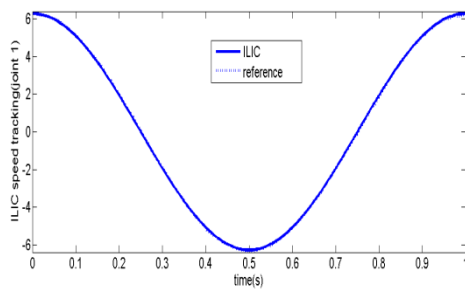


Figure 12. The Speed Tracking Using ILIC of Joint1

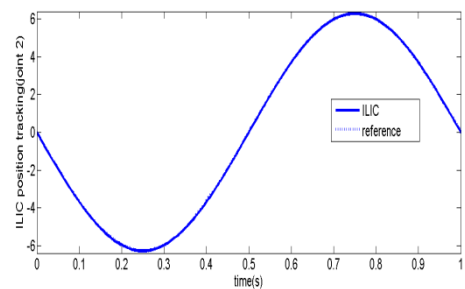


Figure 13. The Speed Tracking Using ILIC of Joint2

For variable force tracking, the desired positions of two joints are $qd1 = \sin(2\pi t)$, and $qd2 = \cos(2\pi t)$. To guarantee the same between desired positions and real outputs at the beginning, the real output is set to be $S(0) = 0$. Applying the control law (5), (6), with the resetting condition and $K_p = 10 \cdot eye(2)$, $\rho = 10$, $M_d = C_d = 1$, $K_d = 0.5$, we get the impedance which is variable with $F_{kd} = \sin(2\pi t)$. The starting state of joint1 and joint2 is $S'(0) = [0 \ 2\pi \ 1 \ 0]^T$, which refers to position and speed of joint1 and joint2. The total iterative times are 8.

4. Discussion

Figure 2-Figure 3 show the constant force tracking results using ILIC and traditional impedance control, respectively. For constant force tracking, using ILIC, the time regulation is less than 0.06S and the overshoot is about 5%, while using traditional control, the time regulation is about 0.09S and the overshoot is about 20%. The steady_state error caused by using ILIC is much smaller than that by using traditional control.

Figure 4-Figure 7 show the variable force tracking results of end-effector after one time iteration, three, five and eight times iterations, respectively. From Figure 4-Figure 7, we can roughly find out the force error converging process of ILIC. The force tracking error of end-effector is large after one time iteration. After two times iterations, the force error becomes smaller. At the eighth time iteration, the force error is nearly zero. Figure 8 shows the force tracking error convergence process of the 8 iterations. The horizontal ordinates denote time, and the vertical coordinates denote force. To simulate the actual situation, we use variable force. It should note that the force refers to end effect force of the two-joint rehabilitation robot. Furthermore, the force should be turned on line according to impaired physical recovery condition. Therefore, it is reasonable to apply variable force, which better meets the actual situations. Fig.9 shows the variable force tracking results using traditional impedance control. From the simulation results, we can find out using traditional control, the force tracking error is $\pm 0.1N$, while using ILIC, the force tracking error is $\pm 0.03N$.

Figure 10-Figure 11 show the position tracking results of joint1 and joint2 using ILIC, respectively. Figure 12-Figure 13 show the speed tracking results of joint1 and joint2 using ILIC, respectively. The position and speed tracking errors tend to zero with the iterative learning, which is small enough to satisfy the requirements. The simulation results show that the proposed ILIC is effective.

Through comparisons of numerical simulation results, the overshoot for constant force tracking is larger than variable force tracking. The reason is the different starting state of position and speed of joints that one is $S'(0) = [0 \ 0 \ 1 \ 0]^T$, and the other is $S'(0) = [0 \ 2\pi \ 1 \ 0]^T$.

Note that, in practical applications, since the joint speed information is estimated by derivative method of position signals from encoders, the measurement noise will accumulate through the iterative process. It is necessary to limit the tracking error and stop iterative learning process.

5. Conclusion

The adaptive ILIC scheme has been proposed for the position and impedance tracking problem of rehabilitation robot with external disturbances. The proposed ILIC was modulated by impaired physical recovery condition, which makes the rehabilitation process more reasonable and effective. Our proposed scheme can improve the effectiveness of rehabilitative training and avoid hurting the impaired limb again. The changes of force and *TTR* were used as inputs of fuzzy controller, and the desired impedance was used as output. Then, we designed adaptive ILIC that was modulated using iterative learning method. The proof of convergence was based upon the use of a Lyapunov-like positive definite sequence, which was shown to be monotonically decreasing under the proposed control scheme. Finally, for two-joint rehabilitation

robot, the simulation experiments of our proposed learning impedance control scheme were compared with that of the traditional impedance control, which confirms the effectiveness of our learning impedance controller.

References

- [1] Colombo, R., Pisano, F., Micera, S., et al. Robotic Techniques for Upper Limb Evaluation and Rehabilitation of Stroke Patients. *IEEE Trans Neural Syst Rehabil Eng.*, 2005; 13(3): 311–324
- [2] Sun, Z.J., Yu, Y., Ge, Y.J., et al. *Research on Sensing Information Forecasting for Power Assist Walking Legs*. ICMA2009;9:1816–1818
- [3] He, J.B., Yi, X.H., Luo, Z.F., Li, G. J.. Backstepping decentralized fault tolerant control for reconfigurable modular robots. *TELKOMNIKA Indonesian Journal of Electrical Engineering*, 2013; 11(7):3508-3516
- [4] Oliveira J L, Reis L P, Faria B M, et al. An Empiric Evaluation of a Real-Time Robot Dancing Framework based on Multi-Modal Events. *TELKOMNIKA Indonesian Journal of Electrical Engineering*. 2012; 10(8):1917-1928.
- [5] Caccavale, F., Siciliano, B., Villani, L. Robot impedance control with nondiagonal stiffness. *IEEE Transactions on Automatic Control*, 1999;44:1943–1946
- [6] Seul Jung, Hsia, T.C., Bonitz, R.G. Force tracking impedance control of robot manipulators under unknown environment., *IEEE Transactions on Control Systems Technology*, 2004;12: 474–483
- [7] Akdoğan, E., Taçgın, E., Adli, M.A. Knee rehabilitation using an intelligent robotic system. *J. Intell. Manuf.* 2009;20: 195–202
- [8] Sang Hoon Kang, Maolin Jin, Pyung Hun Chang. A Solution to the Accuracy/Robustness Dilemma in Impedance Control, *IEEE/ASME Transactions on Mechatronics*, 2009;14: 282–294
- [9] Patel, R.V., Talebi, H.A., Jayender, J., et al. A Robust Position and Force Control Strategy for 7-DOF Redundant Manipulators., *IEEE/ASME Transactions on Mechatronics*, 2009;14: 575– 589
- [10] Tsuji, T., Tanaka, Y. On-line learning of robot arm impedance using neural networks. *Robot Auton. Syst.* 2005;52: 257–271
- [11] Kaneko, K., Horowitz, R. Repetitive and adaptive control of robot manipulators with velocity estimation. *IEEE Transactions on Robotics and Automation*, 1997;13:204–217
- [12] Bukkems, B., Kostic D. , De Jager, B., et al. Learning-based identification and iterative learning control of direct-drive robots. *IEEE Transactions on Control Systems Technology*, 2005;13:537–549
- [13] Xu, J. X., Tan, Y. A. suboptimal learning control scheme for nonlinear systems with time varying parametric uncertainties. *Optimal Control Applications and Methods*, 2001;22: 111–126
- [14] Xu, J. X. The frontiers of iterative learning control C Part II. *International Journal of Systems Control and Information processing*, 2002;46(5): 233–243
- [15] Tayebi, A. Adaptive iterative learning control for robot manipulators, *Automatic*, 2004; 40: 1195–1203
- [16] Visioli, A., Ziliani, G., Legnani, G. Iterative Learning Hybrid Force/Velocity Control for Contour Tracking. *IEEE Transactions on Robotics*, 2010;26:388–393
- [17] Pham Thuc Anh Nguyen, Hyun-Yong Han, Arimoto, S. *Iterative learning of impedance control*. 1999 IEEE/RSJ International Conference on Intelligent Robots and Systems, 1999. IROS '99; 2:653–658
- [18] Tsuji, T., Ito, K., Morasso, P.G. Neural network learning of robot arm impedance in operational space, *IEEE Transactions on Systems, Man, and Cybernetics, Part B: Cybernetics*, 1996;26:290–298
- [19] Chien-Chern Cheah, Danwei Wang. Learning impedance control for robotic manipulators, *IEEE Transactions on Robotics and Automation*, 1998;14:452–46
- [20] Byungchan Kim, Jooyoung Park, Shinsuk Park, et al. Impedance Learning for Robotic Contact Tasks Using Natural Actor-Critic Algorithm, *IEEE Transactions on Systems, Man, and Cybernetics, Part B: Cybernetics*, 2010; 40: 433–443
- [21] Xu, G.Z., Song, A.G., Li, H. J. Adaptive Impedance Control for Upper-Limb Rehabilitation Robot Using Evolutionary Dynamic Recurrent Fuzzy Neural Network. *J Intell Robot Syst* , 2011; 62:501–525
- [22] Toshiro Noritsugu, Toshihiro Tanaka. Application of Rubber Artificial Muscle Manipulator as a Rehabilitation Robot. *IEEE/ASME Transactions on Mechatronics*, 1997;2(4):259–267
- [23] D.J., Bennett, J.M. Hollerbach, Y. Xu, et al. Time varying stiffness of human elbow joint during cyclic voluntary movement. *Experimental Brain Research*, 1992;88(2):433–442
- [24] H. I., Krebs, N. Hogan, M. L., Aisen, and B. T., Volpe. Robot-aided eurorehabilitation. *IEEE Trans. Rehabil. Eng.*, 1998;6(1): 75–87